

NRL Report 8277

12
NW

Currents on Generalized Yagi Structures

WALTER K. KAHN

*Airborne Radar Branch
Radar Division*

LEAL

AD A063374

January 8, 1979

DDC FILE COPY.



DDC
RECEIVED
JAN 18 1979
A

NAVAL RESEARCH LABORATORY
Washington, D.C.

Approved for public release; distribution unlimited.

79 0 10 10 10

SECURITY CLASSIFICATION OF THIS PAGE (When Data Entered)

REPORT DOCUMENTATION PAGE		READ INSTRUCTIONS BEFORE COMPLETING FORM
1. REPORT NUMBER 141 NRL Report-8277	2. GOVT ACCESSION NO.	3. RECIPIENT'S CATALOG NUMBER
4. TYPE (and Subtype)	5. TYPE OF REPORT & PERIOD COVERED 9 Final report on one phase of a continuing NRL project	6. PERFORMING ORG. REPORT NUMBER
7. AUTHOR(s) 10 Walter K. Kahn	8. CONTRACT OR GRANT NUMBER(s)	
9. PERFORMING ORGANIZATION NAME AND ADDRESS Naval Research Laboratory Washington, DC 20375	10. PROGRAM ELEMENT, PROJECT, TASK AREA & WORK UNIT NUMBERS NRL Problems R02-29B and R12-85A Project WF12-141-601	
11. CONTROLLING OFFICE NAME AND ADDRESS Naval Air System Command Washington, DC 20361	12. REPORT DATE 11 January 8, 1979	13. NUMBER OF PAGES 32
14. MONITORING AGENCY NAME & ADDRESS (if different from Controlling Office) 12 33p.	15. SECURITY CLASS. (of this report) UNCLASSIFIED	15a. DECLASSIFICATION/DOWNGRADING SCHEDULE
16. DISTRIBUTION STATEMENT (of this Report) Approved for public release: distribution unlimited 16 F12, 141		
17. DISTRIBUTION STATEMENT (of the abstract entered in Block 20, if different from Report) 17 WF12, 141-601		
18. SUPPLEMENTARY NOTES		
19. KEY WORDS (Continue on reverse side if necessary and identify by block number) Antennas Open periodic structures Yagi-antennas Linear phased arrays Dipole array currents Active impedance Surface-wave antennas Broadband antennas		
20. ABSTRACT (Continue on reverse side if necessary and identify by block number) Characteristics of currents produced on an infinite linear array of parasitic radiators when one of the radiators is excited are found. Yagi antennas use arrays of electric dipoles; detailed analysis and results are given for a generalized Yagi structure in which the dipoles are inclined at an arbitrary angle to the array axis. Calculations are carried out within a network formulation. The integral solution obtained from this formulation is used to demonstrate the interrelation between the properties of the array of radiators excited parasitically or excited as a phased array. The solution simplifies remarkably when the		

DD FORM 1473 1 JAN 73 EDITION OF 1 NOV 68 IS OBSOLETE
S/N 0102-014-6601

SECURITY CLASSIFICATION OF THIS PAGE (When Data Entered)

251 950

→ not a
H

20. Abstract (Continued)

angle of inclination of the dipoles is 54.74 degrees. The surface-wave components and the (feed) correction currents are then explicitly evaluated. Although for conventional Yagi structures surface-wave solutions have been found only for capacitive dipoles, for sufficiently small angles of inclination surface waves can exist on arrays of inductive dipoles.

CURRENTS ON GENERALIZED YAGI STRUCTURES

INTRODUCTION

This report evaluates properties of currents on an infinite linear array of parasitic radiators when one of the radiators is excited. In practical applications Yagi antennas use arrays of parasitic electric dipoles. Therefore the detailed analysis deals with a generalized Yagi (dipole) structure. The structure has been generalized by allowing the dipole antennas to be inclined at an arbitrary angle to the array axis; in a conventional Yagi the dipoles are perpendicular to the array axis.

When the array is excited, the currents at each radiator may be decomposed into a surface-wave component plus a correction component. The surface-wave currents are of particular importance in design, and their wave properties are found for various angles of inclination of the dipoles.

Calculations are carried out within the framework of a network formulation. The integral solution obtained from this formulation is used to demonstrate the interrelation between the properties of the array of short-circuited radiators excited parasitically and those of the *same* structure when each radiator is excited by a real generator, as in a phased array. Analytical (closed) forms previously obtained in phased-array studies are used to eliminate numerical difficulties due to slow convergence of the series which arise in previous treatments of long Yagi antennas. For the special case of dipoles inclined at the angle $\arctan \sqrt{2} = \arcsin \sqrt{2/3} = 54.74^\circ$ to the array axis, the functional form of the solution simplifies remarkably. The surface-wave and (feed) correction currents are then explicitly evaluated, in the complex plane, as a pole-residue contribution and a branch-cut contour integral.

As recounted by Professor Uda [1,2], the Yagi-Uda antenna was invented in 1926. Further practical and theoretical studies were undertaken, but, as noted by Ehrenspeck and Poehler [3], in the late 1960's there existed no rigorous solution of the Yagi problem. The experimental results were restricted to special cases, with no attempt made to find a connection between them. Ehrenspeck and Poehler developed general design principles for long Yagi antennas. Their experiments demonstrated the dominant role played by the surface-wave parameters in determining the performance of this antenna. This is now well understood within the context of surface-wave antenna design [4].

The variation of the phase velocity of the surface wave on infinite Yagi structures was analyzed by Sengupta [5]. Mailloux [6,7] provided a complete solution, including excitation coefficient, for the infinite Yagi structure excited at one element of the structure. He then applied these results to finite Yagi arrays, obtaining excellent agreement with experiment and with an alternative theory for such arrays by King and Sandler [8]. Gately et al. [9] showed that a comparatively simple calculation which treats the dipoles of the Yagi

array as minimum-scattering antennas [10,11] also yields similar results for finite arrays. For any *given* array configuration, even if it includes a large number of elements, such direct calculations of radiation from a finite array no doubt now provide the most convenient route to accurate results. On the other hand, because of the many variables, estimates for appropriate designs continue to be most readily derived from the surface-wave point of view.

In the next section of this report the problem posed by a linear array of identical parasitic radiators is given a generic network formulation. A formal solution in the form of an integral is obtained for the currents produced on such a structure when a single element is excited (the Green's function currents.) The technique for solution was described by Mailloux [6] and follows closely that employed in the analysis of phased arrays [12,13]. In the present report it is shown that the active impedance (the input impedance to any antenna element when all are excited with uniform amplitude and uniform phase difference ξ) is intimately connected with the surface-wave parameters. In particular, surface waves can occur only for values of ξ denoted ξ_s corresponding to the "invisible region" in phased-array parlance. For such values no radiation occurs, and the active impedance is reactive. The ratio of surface-wave velocity to the velocity of light is kD/ξ_s , where kD is the element spacing in electrical radians and ξ_s is a zero of an active impedance as a function of phasing angle. It would seem that analyses carried out on a variety of phased-array structures can now be turned to account in the design of surface-wave antennas.

In Refs. 12 and 13 Wasyliwskyj and Kahn analyzed an infinite linear array consisting of dipoles (minimum-scattering antennas) oriented at an arbitrary angle with respect to the array axis. An essentially closed form for the active impedance is available from Ref. 12. This form simplifies remarkably for dipoles inclined at the angle $\theta_0 = \arcsin \sqrt{2/3} = \arctan \sqrt{2}$. The special nature of this angle for dipoles was first noted by Hazeltine [14].* The third section of this report is devoted to the Yagi structure consisting of dipoles inclined at this special angle. For this case the formal integral solution can be evaluated by contour integration in the complex plane. The surface-wave components of currents at the antenna terminals are evaluated as pole-residue contributions, and the remaining components of current are evaluated as branch-cut integrals. On the infinite structure these branch-cut "correction" or space-wave components of current are the only ones giving rise to radiation away from the structure. In contrast to the surface-wave components, which retain a constant amplitude along the structure, the correction components decrease with distance for antenna elements removed from the one excited. It is found that this decrease is at least as rapid as $1/n$, where n is number of elements removed from the excited element. In a Yagi array this type of current would be responsible for "feed radiation."

*Hazeltine [14] discovered that the static coupling between parallel magnetic coils (more generally dipoles) was eliminated when the coils are inclined to a line connecting their centers at the special angle $\theta_0 = \arctan \sqrt{2}$. Not only the static coupling term inversely proportional to the cube of the coil separation but also a dynamic term inversely proportional to the square of the separation are eliminated. Only the dynamic radiation term inversely proportional to the separation remains. The author is grateful to Dr. Harold A. Wheeler for bringing Hazeltine's discovery to his attention. (Dr. Wheeler has discussed Hazeltine's discovery in a recent book *Hazeltine the Professor*, published by the Hazeltine Corporation, Greenlawn, N. Y., in 1978.)

The last section deals with the parameters of surface-wave components on the generalized dipole Yagi structures. On the one hand, except at the one special angle treated in the third section, the complexity of the integrand in the formal solution would seem to preclude a corresponding complete evaluation. On the other hand the form obtained for the active impedance [12] is convenient for computation. Consequently it becomes economical to compute the actual variation of surface-wave parameters with frequency for any particular structure of interest. Examples of such calculations are given. For conventional Yagi structures ($\theta_0 = 90^\circ$) surface-wave solutions have been found only for capacitive (short) dipoles. It is shown that, for sufficiently small angle of inclination θ_0 , surface waves can also exist on arrays of inductive dipoles. In the computations the mutual coupling between antennas is (apart from a scale factor) approximated as the coupling between minimum scattering antennas having radiation patterns of short dipoles. Therefore results obtained for inductive dipoles apply, strictly speaking, to short inductively loaded dipoles. Because of the slow change of the radiation pattern, the theory of mutual coupling between minimum scattering antennas indicates that these results approximately apply to arrays of (unloaded) dipoles somewhat longer than $1/2$ wavelength.

NETWORK FORMULATION

An infinite array of identical antennas uniformly spaced along a straight line or axis is characterized at the terminals of the antennas by voltages V_m and currents I_n , where the subscripts denote the m th and n th antennas. These terminal quantities are related by the open-circuit impedance coefficients Z_{mn} :

$$V_m = \sum_{n=-\infty}^{\infty} Z_{mn} I_n. \quad (1)$$

In view of the symmetry of this array, the impedance coefficients depend only on the separation between the m th and n th antennas $(n - m)D$, where D is the separation of adjacent antennas. Thus Z_{mn} is a function of only the difference

$$\nu = n - m. \quad (2)$$

Lorentz reciprocity in the electromagnetic field implies that the matrix of impedance coefficients is symmetrical:

$$Z_{mn} = Z_{nm}. \quad (3)$$

It follows that

$$Z_{mn} = Z_\nu = Z_{-\nu}. \quad (4)$$

The basic network relation (1) can therefore be rewritten as

$$V_m = \sum_{\nu=-\infty}^{\infty} Z_\nu I_{m+\nu}. \quad (5)$$

This is an infinite-order, linear, finite-difference equation.

Let us assume that only one of the antennas, the ℓ th antenna, is excited by a voltage generator E_g with internal reactance X_a (Fig. 1). The remaining antennas are each terminated in a like reactance X_a ; they are excited only parasitically through mutual coupling. These conditions constrain the terminal voltages and currents to

$$V_m = E_g \delta_{m\ell} - j X_a I_m, \quad (6)$$

where $\delta_{m\ell}$ is the Kronecker delta:

$$\delta_{m\ell} = 1, \quad m = \ell, \quad (7a)$$

$$= 0, \quad m \neq \ell. \quad (7b)$$

When these constraints are inserted into the difference equation (5), the result is

$$E_g \delta_{m\ell} = \sum_{\nu=-\infty}^{\infty} (Z_\nu + j X_a \delta_{0\nu}) I_{m+\nu}. \quad (8)$$

To solve the difference equation (8), one can introduce the Fourier transform of the currents I_ν :

$$g(\xi) = \sum_{\nu=-\infty}^{\infty} I_\nu e^{j\nu\xi} \quad (9a)$$

and, inversely,

$$I_\nu = \frac{1}{2\pi} \int_{-\pi}^{\pi} g(\xi) e^{-j\nu\xi} d\xi, \quad (9b)$$

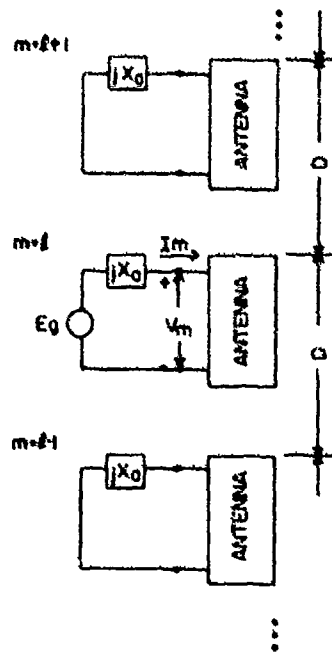


Fig. 1 — Infinite array of identical antennas, with one antenna excited

From this definition it follows that the Fourier transform of the currents $I_{m+\nu}$ is $e^{-jm\xi} \mathcal{J}(\xi)$:

$$I_{m+\nu} = \frac{1}{2\pi} \int_{-\pi}^{\pi} [\mathcal{J}(\xi) e^{-j\nu\xi}] e^{-jm\xi} d\xi. \quad (10)$$

The Kronecker delta is given by

$$\delta_{m\ell} = \frac{1}{2\pi} \int_{-\pi}^{\pi} e^{-j(m-\ell)\xi} d\xi. \quad (11)$$

On insertion of the integral representations (10) and (11), difference equation (8) becomes

$$\frac{1}{2\pi} \int_{-\pi}^{\pi} E_g e^{-j(m-\ell)\xi} d\xi = \sum_{\nu=-\infty}^{\infty} (Z_\nu + jX_a \delta_{0\nu}) \frac{1}{2\pi} \int_{-\pi}^{\pi} \mathcal{J}(\xi) e^{-j(m+\nu)\xi} d\xi. \quad (12)$$

Interchanging the order of summation and integration and equating the resultant transforms, one may solve for $\mathcal{J}(\xi) = \mathcal{J}^{(\ell)}(\xi)$:

$$\mathcal{J}^{(\ell)}(\xi) = \frac{E_g e^{j\ell\xi}}{jX_a + Q(\xi)}, \quad (13)$$

where

$$Q(\xi) = \sum_{\nu=-\infty}^{\infty} Z_\nu e^{-j\nu\xi}. \quad (14)$$

The superscript ℓ makes explicit the dependence of the solution on excitation at the port of the ℓ th antenna only. The currents $I_n^{(\ell)}$ which constitute the solution of (8) (in effect a Green's function solution) may then be recovered from (13):

$$I_n^{(\ell)} = \frac{1}{2\pi} \int_{-\pi}^{\pi} \frac{E_g e^{-j(n-\ell)\xi}}{jX_a + Q(\xi)} d\xi. \quad (15)$$

It is clear from (15) that the properties which distinguish the terminal currents on one particular array from those on another reside entirely in X_a and the functional form of $Q(\xi)$ [15]. From symmetry considerations or from (15)

$$I_n^{(\ell)} = I_{n-\ell}^{(0)}. \quad (16)$$

In the rest of this report the superscript ℓ will be suppressed by setting $\ell = 0$.

In the phased-array literature [12,16,17] $Q(\xi)$ is identified as the active impedance, which is the input impedance at any element of the infinite array when all elements are excited by generators of uniform amplitude and constant phase difference (ξ radians). Therefore an

infinite connection exists between the characteristics of the parasitic array and those of the same array of antennas employed as an active phased array. The implications of this connection will be developed subsequently.

A significant difficulty arises in the evaluation of the currents I_n from (15) when the integrand has singularities for values of ξ in the interval $-\pi < \xi < \pi$. As will be discussed from several points of view, particular singularities contribute surface-wave components of current. These particular singularities occur at the roots $\xi_s^{(p)}$ of

$$jX_a + Q(\xi) = 0. \quad (17)$$

Clearly a necessary condition for occurrence of a root in (17) is that the real part of the active impedance $Q(\xi)$ vanish:

$$\text{Re } Q(\xi) = 0. \quad (18a)$$

It is well known that for closely spaced arrays, $0 < kD < \pi$, symmetry considerations dictate a range of values of ξ in which (18a) holds, the so-called "invisible" region of phasing angles [12,16,17]

$$kD < |\xi| < \pi. \quad (18b)$$

Therefore real roots of (17) quite generally lie in that range. Further, it can be shown that, due to the reciprocity conditions (3) and (4), these roots occur in pairs with opposite sign (Appendix). If $\xi_s^{(p)}$ is a real root of (17), then $-\xi_s^{(p)}$ is also a root, which will be denoted

$$\xi_s^{(-p)} = -\xi_s^{(p)}, \quad p = \pm 1, \pm 2, \dots \quad (19)$$

Surface-wave components of current (components that maintain a constant magnitude from one antenna element to the next and a constant phase difference from one element to the next) are found on closely spaced arrays. These waves have phase velocity

$$v_s^{(p)} = \frac{\omega D}{\xi_s^{(p)}} = c \frac{kD}{\xi_s^{(p)}}, \quad (20)$$

where c is the velocity of light. In view of (18b) they are "slow waves."

The total currents I_n are conveniently dissected into surface-wave and correction components

$$I_n = I_{sn} + I_{cn}, \quad (21a)$$

where

$$I_{sn} = I_{s0} |k_s^{-1}|. \quad (21b)$$

I_{sn} is by definition a surface-wave component of current (with the superscript p being omitted, because only one surface wave is assumed for simplicity). The absolute value in

(21b) is justified by the symmetry of the problem. The unknown amplitude I_{s0} can be determined from the Fourier transform of (21a)

$$g(\xi) = g_s(\xi) + g_c(\xi), \quad (22a)$$

where

$$g_s(\xi) = I_{s0} \sum_{n=-\infty}^{\infty} e^{-j|n|\xi_s + jn\xi} = I_{s0} \left(-1 + \frac{1}{1 - e^{-j(\xi + \xi_s)}} + \frac{1}{1 - e^{j(\xi - \xi_s)}} \right), \quad (22b)$$

with the requirement that $g_c(\xi)$ be nonsingular at $\xi = \xi_s$ [6]. If no other (type of) singularities are present, the currents I_{cn} may then be evaluated straightforwardly from $g_c(\xi)$ and the inverse transform (9b). When other types of singularities do occur, these must be examined. If they are integrable, no further analytical difficulties (but quite possibly further numerical difficulties) may be involved in the evaluation of I_{cn} :

$$I_{cn} = \frac{1}{2\pi} \int_{-\pi}^{\pi} g_c(\xi) e^{-jn\xi} d\xi. \quad (22c)$$

An alternative means for evaluation of the currents is accessible when the analytical properties of $Q(\xi)$ can be determined in detail. Extension of $Q(\xi)$ into the complex ζ plane

$$\zeta = \eta e^{j\xi}, \quad \eta > 0, \quad (23)$$

brings with it the elegance and power of function-theoretic techniques for integration. As a function of the complex variable ζ , the active impedance function will be denoted by $q(\zeta)$. When $\eta = 1$,

$$q(\zeta) = q(\eta e^{j\xi}) = Q(\xi). \quad (24)$$

The currents I_n are then given by the contour-integral formula

$$I_n = \frac{1}{2\pi j} \int_C \frac{E_g \zeta^{-(n+1)}}{jX_a + q(\zeta)} d\zeta, \quad (25)$$

which is equivalent to (15) when C is the unit circle in the ζ plane, properly indented about any singularities. The proper indentations may be determined by introducing a small amount of dissipation (which moves the singularities off the unit circle) and then passing to the limit of zero loss [4]. An example of such a contour will be shown in Fig. 4a in connection with the particular case of inclined dipoles considered in the next section.

When the integral (25) is evaluated by deforming the contour C about the singularities of the integrand, the residue contribution, due to a simple pole at $\zeta = \zeta_s$ on the unit circle, is readily identified as a surface-wave current. In general

$$I_{sn} = E_g \left. \frac{\zeta^{-(n+1)}}{\frac{d}{d\zeta} q(\zeta)} \right]_{\zeta = \zeta_s} \quad (26a)$$

$$= j E_g \left. \frac{e^{-jn\xi}}{\frac{d}{d\xi} Q(\xi)} \right]_{\xi = \xi_s} \quad (26b)$$

The preceding formulation is readily generalized to an infinite array of a given complex of antennas [13]. The given complex, termed a subarray of antennas, may comprise one or more multiport antennas (Fig. 2) or simply an ordinary subarray of several identical one-port antennas. Suppose the antennas in each subarray have M input ports. Then the impedance coefficients of the infinite structure may be denoted by $Z_{\bar{m}\bar{n};mn}$, $\bar{m}, \bar{n} = 1, 2, \dots, M$, where, for example, \bar{m} identifies the \bar{m} th port of the m th subarray. The Lorentz reciprocity condition (3) is then replaced by

$$Z_{\bar{m}\bar{n};mn} = Z_{\bar{n}\bar{m};nm} \quad (27a)$$

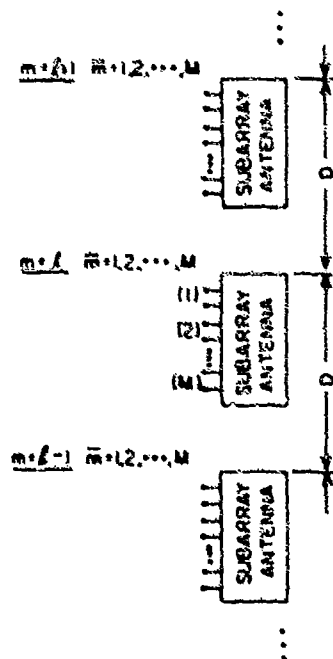


Fig. 2 - Array of subarray antennas

With the adoption of matrix notation within the subarray,

$$\underline{\underline{Z}}_{mn} = \tilde{\underline{\underline{Z}}}_{nm}, \quad (27b)$$

where $\tilde{\underline{\underline{Z}}}_{nm}$ denotes the transpose of the M -by- M matrix $\underline{\underline{Z}}_{nm}$. From symmetry (2) it follows that

$$\underline{\underline{Z}}_{mn} = \underline{\underline{Z}}_{\nu} = \tilde{\underline{\underline{Z}}}_{-\nu}. \quad (28)$$

Accordingly the basic network relation can be written as

$$\underline{V}_m = \sum_{\nu=-\infty}^{\infty} \underline{\underline{Z}}_{\nu} \underline{I}_{m+\nu}, \quad (29)$$

where \underline{V}_m and \underline{I}_n are M -dimensional column matrices:

$$\tilde{\underline{V}}_m = \left[V_{1;m} \ V_{2;m}, \dots, V_{M;n} \right] \quad (30a)$$

and

$$\tilde{\underline{I}}_n = \left[I_{1;n} \ I_{2;n}, \dots, I_{M;n} \right]. \quad (30b)$$

The solution of (29) proceeds in a fashion entirely parallel to the solution of (5). In particular

$$\underline{I}_n^{(l)} = \frac{1}{2\pi} \int_{-\pi}^{\pi} \left[j\underline{\underline{X}}_a + \underline{\underline{Q}}(\xi) \right]^{-1} \underline{E}_g e^{-j(n-l)\xi} d\xi \quad (31)$$

is obtained parallel with (15). Surface-wave currents may occur and are again attributable to singularities of the integrand in (31), that is, to real roots $\xi_s^{(l)}$ of the determinant:

$$\det \left[j\underline{\underline{X}}_a + \underline{\underline{Q}}(\xi) \right] = 0. \quad (32)$$

APPLICATION TO AN INFINITE ARRAY OF INCLINED DIPOLES

An infinite, uniform, linear array of electric dipoles, each inclined at angle θ_0 to the array axis, is shown in Fig. 3a. Let the input impedance to one of the dipole antennas taken from the array be

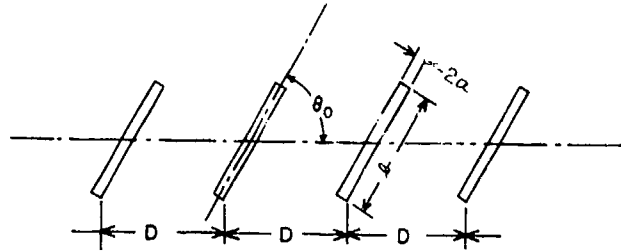


Fig. 3a - Infinite linear array of metal rods (radius a and length b) or short-circuited electric dipole antennas

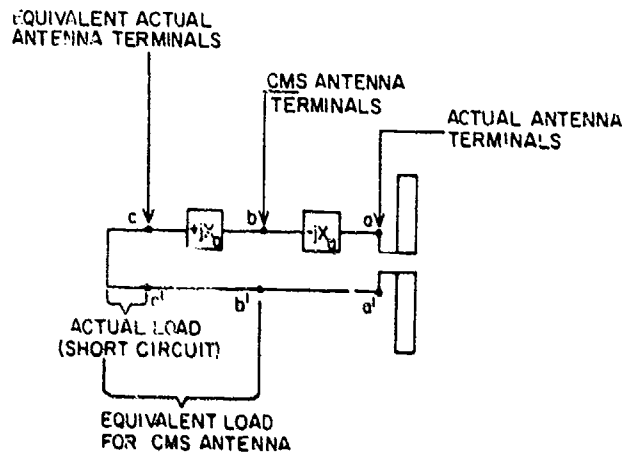


Fig. 3b - Dipole and equivalent canonical-minimum-scattering (CMS) antenna circuit

$$\hat{Z}_a = \hat{R}_a + j\hat{X}_a \quad (33)$$

in free space. To use theory developed for minimum-scattering antennas to calculate mutual impedance [9,11,17], each antenna is modified through the addition of the series reactance circuit shown in Fig. 3b. At terminal bb' each dipole is closely modeled by a canonical-minimum-scattering (CMS) antenna with input impedance R_a . Terminals cc' are in all respects equivalent to the original antenna terminals aa' . With respect to the terminals bb' the impedance coefficients for the array, normalized to R_a , are given by [11,12]

$$Z_\nu = \frac{3}{2} \left[h_0^{(2)}(kD|\nu|) - \frac{h_1^{(2)}(kD|\nu|)}{kD|\nu|} \right] \sin^2 \theta_0 + 3 \frac{h_1^{(2)}(kD|\nu|)}{kD|\nu|} \cos^2 \theta_0, \quad \nu \neq 0, \quad (34a)$$

$$= 1, \quad \nu = 0, \quad (34b)$$

where the particular spherical Hankel functions are [18]

$$h_0^{(2)}(z) = j \frac{e^{-jz}}{z} \quad (35a)$$

and

$$h_1^{(2)}(z) = -\frac{e^{-jz}}{z} \left(1 - j \frac{1}{z}\right) \quad (35b)$$

and where $k = 2\pi/\lambda$, D is the distance between adjacent dipole centers, and $D|\nu| = D|n - m|$ is the distance between the m th and n th dipole centers. It was noted following (1) that the mutual impedance depends only on the distance between the m th and n th dipole centers and thus on $kD|m - n| = kD|\nu|$. Impedance quantities without the caret are normalized to R_a .

An infinite Yagi structure is obtained when the dipoles are short-circuited at the terminals aa' of the antennas. Putting the short circuit at the terminals cc' shows that the Yagi structure is equivalent to the array of CMS antennas at terminals bb' terminated in reactances X_a . When an ideal generator is placed in series with this reactance at one of the antennas, the problem of finding the terminal currents at all antennas is a particular example of the network problem formally solved in the preceding section. As was pointed out in that section, the features distinguishing various infinite Yagi structures are concentrated in the functional form of the active impedance $Q(\xi)$ for all phasing angles ξ , $-\pi < \xi < \pi$, given by Eq. (14). A highly convergent form of this impedance was previously obtained by Wasyliwskyj and Kahn [12].

When the dipoles are inclined to the array axis at the special angle

$$\sin^2 \theta_0 = \frac{2}{3}, \quad (36)$$

the mutual impedance (34a) simplifies to [12,14*]

$$Z_{\nu} = h_0^{(2)}(kD|\nu|). \quad (37)$$

The active impedance is then given by the closed form

$$Q(\xi) = \frac{\pi}{kD} - \frac{j}{kD} \ln \left[2 |\cos kD - \cos \xi| \right], \quad 0 < |\xi| < kD, \quad (38a)$$

$$= -\frac{j}{kD} \ln \left[2 |\cos kD - \cos \xi| \right], \quad kD < |\xi| < \pi. \quad (38b)$$

For dipoles spaced more than 1/2 wavelength apart ($kD > \pi$) the active impedance has a nonvanishing real part for all values of ξ . All surface-wave roots $\xi_s^{(p)}$ of (17) can therefore be found** using (38b):

$$\cos \xi_s^{(p)} = \cos kD - \frac{1}{2} \exp(kDX_a). \quad (39)$$

*Footnote on page 2.

**Sengupta [5] derived a similar form. However, his result was intended as an approximation for roots of the conventional Yagi structure, with $\theta_0 = \pi/2$.

In the preceding section (Eq. (25)) the general solution for the currents I_n was formulated as a contour integral in the complex $\zeta = \eta e^{j\xi}$ plane:

$$I_n = \frac{1}{2\pi j} \int_C \frac{E_g \zeta^{-(n+1)}}{+jX_a + q(\zeta)} d\zeta. \quad (40a)$$

Here

$$q(\zeta) = \frac{-j}{kD} \text{Ln}(1 - \sigma\zeta) + 1 - \frac{j}{kD} \text{Ln}\left(1 - \frac{\sigma}{\zeta}\right) \quad (40b)$$

$$= 1 - \frac{j}{kD} \text{Ln} \left\{ \sigma \left[\left(\sigma + \frac{1}{\sigma}\right) - \left(\zeta + \frac{1}{\zeta}\right) \right] \right\}, \quad (40c)$$

in which

$$\sigma = e^{-jkD}, \quad (40d)$$

with $q(\zeta)$ representing the continuation of (38) into the complex ζ plane, the contour C being the unit circle $|\zeta| = 1$ indented as shown in Fig. 4a, and the notation $\text{Ln } \zeta'$ denoting the principal branch of the natural logarithm function:

$$\text{Ln } \zeta' = \ln \eta' + j\xi', \quad -\pi < \xi' \leq \pi. \quad (41)$$

The active impedance function $q(\zeta)$, and consequently the integrand in (40a), has four branch points, at

$$\zeta = \infty, \sigma, \frac{1}{\sigma}, 0. \quad (42)$$

The branch cuts, corresponding to (41), have been chosen to run between ∞ and σ and between $1/\sigma$ and 0 . The integrand also has poles at the zeros of the denominator $\zeta_s^{(p)} = e^{jk_s^{(p)}}$, given by (39), and at a pole of the numerator which occurs at infinity when $n < -1$. The contour C is indented about the branch points only to avoid ambiguities in the drawing, since the singularities at these points are integrable. On the other hand, the indentations at the surface-wave poles $\zeta_s^{(p)}$ are essential and are dictated by uniqueness of the solution for the currents. A detailed discussion of these points is contained in the Appendix.

Preparatory to evaluating the integral in (40a), the contour C may be deformed about the singularities of the integrand as shown in Fig. 4b for $n \geq 0$ and as shown in Fig. 4c for $n < 0$. In either case the integral naturally separates into the two components given by (21a). A surface-wave contribution I_{sw} arises from the pole, and a correction contribution I_{cb} arises from integration around the branch cut. For $n \geq 0$ the circular arc of large radius in Fig. 4b does not contribute.

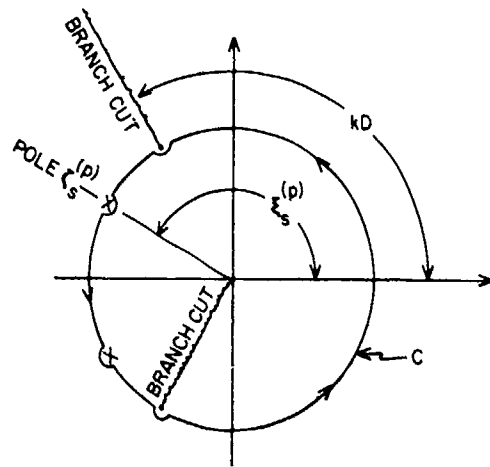


Fig. 4a - Contour of integration C , indented around singularities on the unit circle

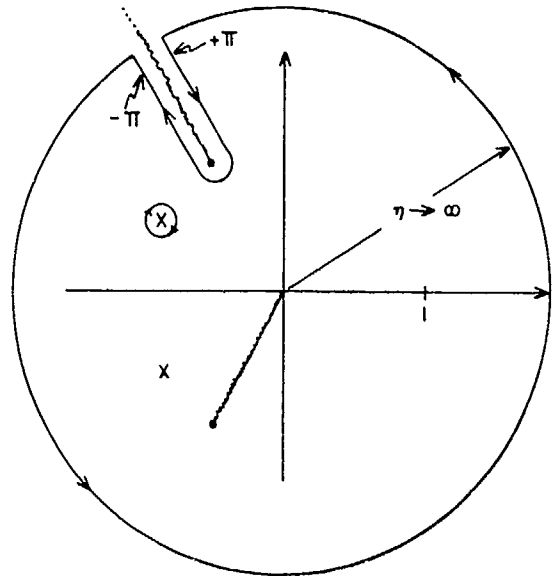


Fig. 4b - Deformed contour equivalent to C in Fig. 4a when $n \geq 0$

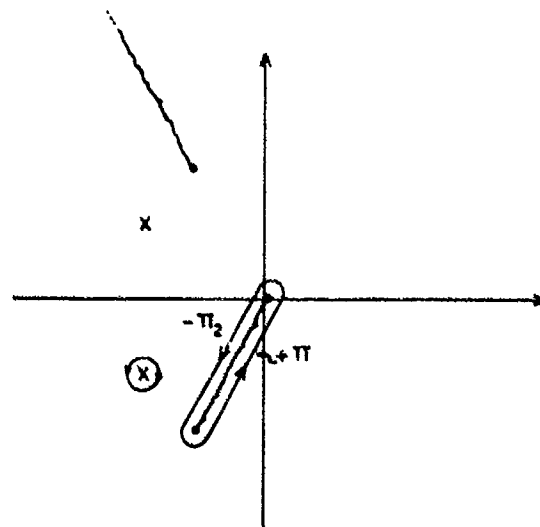


Fig. 4c - Deformed contour equivalent to C in Fig. 4a when $n < 0$

The general form of the contributions due to the (simple) poles has already been stated as (26a) or (26b). Substitution in (26a) of the active impedance function (40c) or substitution in (26b) of the active impedance (38b) for the dipoles inclined at the special angle (36) yields

$$I_{sn} = -\text{sgn}(p)E_g(kD)e^{-jn\xi_s^{(p)}} \left[\frac{\cos kD - \cos \xi_s^{(p)}}{\sin \xi_s^{(p)}} \right]. \quad (43)$$

The function

$$\begin{aligned} \text{sgn}(p) &= +1, p > 0, \\ &= -1, p < 0, \end{aligned}$$

accounts for the sense in which the contour circling the pole is traced. In view of the relation (19) which is verified by (39)

$$I_{sn} = I_{s(-n)}, \quad (44)$$

as expected from symmetry.

The integral around the branch cuts must be evaluated numerically. For $n \geq 0$ an appropriate form is readily obtained by use of (40b) and the relations

$$\text{Ln}(1 - \sigma\zeta) = \ln(\eta - 1) + j\pi, \quad \infty > \eta > 1, \quad (45a)$$

for the inward portion of the path of integration and

$$\text{Ln}(1 - \sigma\zeta) = \ln(\eta - 1) - j\pi, \quad 1 < \eta < \infty, \quad (45b)$$

for the outward portion. The result is

$$I_{cn} = \frac{E_g e^{-jnkD}}{2\pi j} \int_1^\infty \left[\frac{\eta^{-n-1}}{\left(1 - \frac{\pi}{kD}\right) + jX_a - j\frac{1}{kD} \text{Ln}\left[(\eta - 1)\left(1 - \frac{\sigma^2}{\eta}\right)\right]} - \frac{\eta^{-n-1}}{\left(1 + \frac{\pi}{kD}\right) + jX_a - j\frac{1}{kD} \text{Ln}\left[(\eta - 1)\left(1 - \frac{\sigma^2}{\eta}\right)\right]} \right] d\eta. \quad (46)$$

For $n > 0$ it is easy to estimate the variation of I_{cn} . The denominators in (46) are $jX_a + q(\zeta)$ evaluated near the branch cut. Each denominator has some finite minimum absolute value

independent of n . It does not take on the value zero; that value occurs only at the roots $\xi_s^{(p)}$. Integration then yields

$$|I_{cn}| \leq \left| \frac{E_g A}{2\pi n} \right|, \quad n > 0, \quad (47)$$

where A is independent of n . Thus $|I_{cn}|$ decreases at least as fast as $1/n$.

For $n < 0$ the integrand diverges as $\xi \rightarrow \infty$. It is convenient to deform the contour C as shown in Fig. 4c. An appropriate form of the branch-cut integral is readily formulated by use of (40b) and the relations

$$\text{Ln} \left(1 - \frac{\sigma}{\xi} \right) = \ln(1 - \eta) + j\pi, \quad 1 > \eta > 0, \quad (48a)$$

for the inward portion of the path of integration and

$$\text{Ln} \left(1 - \frac{\sigma}{\xi} \right) = \ln(1 - \eta) - j\pi, \quad 0 < \eta < 1, \quad (48b)$$

for the outward portion of the path of integration. The result is

$$I_{cn} = \frac{E_g e^{+jn k D}}{2\pi j} \int_0^1 \left\{ \frac{\eta^{-n-1}}{\left(1 - \frac{\pi}{kD}\right) + jX_a - j\frac{1}{kD} \text{Ln} \left[\left(\frac{1}{\eta} - 1\right) (1 - \sigma^2 \eta) \right]} - \frac{\eta^{-n-1}}{\left(1 + \frac{\pi}{kD}\right) + jX_a - j\frac{1}{kD} \text{Ln} \left[\left(\frac{1}{\eta} - 1\right) (1 - \sigma \eta) \right]} \right\} d\eta. \quad (49)$$

Integration then yields

$$|I_{cn}| \leq \left| \frac{E_g B}{2\pi n} \right|, \quad n < 0, \quad (50)$$

where B is independent of n . Thus $|I_{cn}|$ again is shown to decrease at least as fast as $1/n$. In view of symmetry only one of the integrals in (46) and (49) need be evaluated. In fact, using the transformation $\bar{\eta} = 1/\eta$, one verifies directly that

$$I_{cn} = I_{c(-n)}. \quad (51)$$

The currents I_{fn} and I_{cn} were computed for a Yagi structure consisting of an array of dipole antennas inclined to the array axis at the special angle $\theta_0 = 54.74^\circ$ and spaced $D = 0.200$ m apart. Each dipole has length $b = 0.400$ m and radius $a = 0.00635$ m. Absolute lengths are specified to emphasize that the curve shows the true frequency dependence of a Yagi structure of fixed geometry. Of course this structure can be scaled in the usual way from the assumed frequency or design wavelength of 1 m. The dipole radius was selected to

allow comparison of the results of the next section, for $\theta_0 = 90^\circ$, with those of Mailloux. The normalized self-reactance of the dipole X_a has been taken from Jordan [19,20]. The input reactance is normalized by dividing by the input resistance. This normalized value is the same whether referred to the loop or the base (center) of the antenna. The formulas for the antenna impedance are summarized in the next section by (53) and (54). Significant current ratios are plotted in Fig. 5 for a range of free-space wavelengths around 1 m ($kD = 1.257$).

At 1 m or less the self-reactance of the dipole is high, allowing only small parasitic currents to be induced on the dipole structure. The surface-wave currents, such as do exist, propagate at nearly free-space velocity. At higher frequencies ($kD > 1.257$) the dipoles approach resonant length. The lower self-reactance allows high currents to be induced on the dipoles. The surface wave is strongly coupled to the slow-wave structure and propagates at a

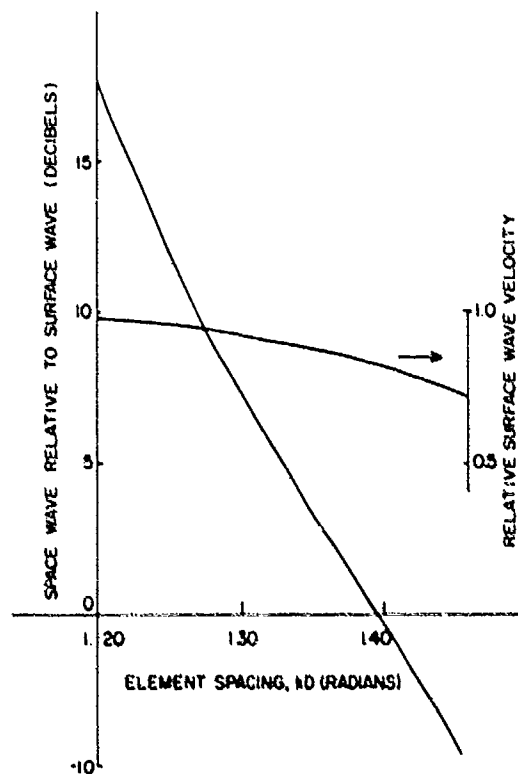


Fig. 5 — Space-wave (correction) component of the current relative to the surface-wave component at the feed point and the relative surface-wave velocity, computed for an infinite array of dipoles inclined at $\theta_0 = \arctan \sqrt{2} = 54.74^\circ$ with dipole radius $a = 0.00835$ m, dipole length $b = 0.400$ m, and dipole spacing $D = 0.200$ m

velocity much below free-space velocity.* The unattenuated surface-wave component of the current becomes large relative to the space-wave component, which in addition decays away from the excited element. The rate of decay of the space-wave component of current is shown in Fig. 6. It is seen to be slightly more rapid than the lower bound $1/n$ developed in (47) and (50).

SURFACE-WAVE CURRENTS ON GENERALIZED INFINITE YAGI STRUCTURES

In this section the dispersion characteristics of the surface-wave currents on arrays of arbitrarily oriented dipoles will be computed. As in the case of the specially inclined dipoles

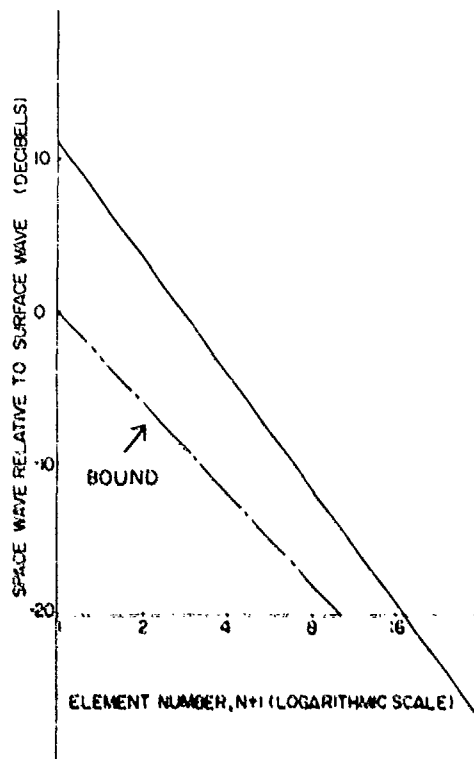


Fig. 6 -- Decay along the Yagi structure of the space-wave component of the current relative to the surface-wave component, computed for an infinite array of inclined dipoles with the same θ_0 , a , b , and D as in Fig. 5 and for a free-space wavelength of 1 m ($kD = 1.257$)

*The characteristics of the surface waves are also found by interpolating for $\theta_0 = 54.74^\circ$ on the wavenumber diagram to be presented as Fig. 7. The slope of a line from the origin to a point on a dispersion curve is the relative phase velocity of the corresponding surface wave v_g/c , given by (20).

of the preceding section, the generally oriented dipoles are easily covered by the network formulation given in the second section. The currents excited by any one driven dipole are given by (15), and the dispersion relation for the surface-wave components is given by (17). Nevertheless analytical difficulties arise due to the increased complexity of the active impedance $Q(\xi)$. Although these difficulties stand in the way of a complete solution along the lines obtained in the preceding section, the dispersion relation is readily solved numerically for the surface-wave parameters.

When the more general expression for the mutual impedance (34a) is substituted into the formula for the active impedance (14), the resulting series may be summed by an extension of the methods employed in the Appendix. This sum, found in Ref. 12, is

$$\operatorname{Re} Q(\xi) = \frac{3\pi}{2kD} \left(1 - \frac{\xi^2}{(kD)^2}\right) \left(\cos^2 \theta_0 - \frac{1}{2} \sin^2 \theta_0\right) + \frac{3\pi}{2kD} \sin^2 \theta_0, \quad |\xi| < kD < \pi, \quad (52a)$$

$$= 0, \quad kD < |\xi| < \pi, \quad (52b)$$

and

$$\operatorname{Im} Q(\xi) = u(\xi) \left(\cos^2 \theta_0 - \frac{1}{2} \sin^2 \theta_0\right) + w(\xi) \sin^2 \theta_0, \quad (52c)$$

where

$$u(\xi) = \frac{3}{(kD)^3} \left[2.404 + \int_0^{kD-\xi} (kD - \xi - x) \ln 2 \sin \frac{x}{2} dx + \int_0^{kD+\xi} (kD + \xi - x) \ln 2 \sin \frac{x}{2} dx \right. \\ \left. - \frac{3}{(kD)^2} \int_0^{kD+\xi} \ln 2 \sin \frac{x}{2} dx + \int_0^{kD-\xi} \ln 2 \sin \frac{x}{2} dx \right], \quad |\xi| < kD < \pi, \quad (52d)$$

$$= \frac{3}{(kD)^3} \left[2.404 + \int_0^{\xi-kD} (\xi - kD - x) \ln 2 \sin \frac{x}{2} dx + \int_0^{\xi+kD} (\xi + kD - x) \ln 2 \sin \frac{x}{2} dx \right. \\ \left. - \frac{3}{(kD)^2} \left[\int_0^{\xi+kD} \ln 2 \sin \frac{x}{2} dx - \int_0^{\xi-kD} \ln 2 \sin \frac{x}{2} dx \right] \right], \quad kD < |\xi| < \pi, \quad (52e)$$

and (with a factor 3/2 added that is missing in Ref. 12)

$$w(\xi) = \frac{3}{2kD} \ln 2 (\cos \xi - \cos kD), \quad |\xi| < kD < \pi, \quad (52f)$$

$$= \frac{3}{2kD} \ln 2 (\cos kD - \cos \xi), \quad kD < |\xi| < \pi. \quad (52g)$$

The reactance of the dipole \hat{X}_a may be obtained by any independent means. Herein results quoted from Jordan and Balmain [19,20] are used. Within the approximations employed for mutual coupling, the physical dimensions of the dipole (length and radius) enter only through the value of the input impedance $\hat{R}_a + j\hat{X}_a$:

$$\frac{1}{2}\hat{R}_a = 15[(2 + 2 \cos \hat{b}) S_1(\hat{b}) - (\cos \hat{b}) S_1(2\hat{b}) - 2(\sin \hat{b}) Si(\hat{b}) + (\sin \hat{b}) Si(2\hat{b})] \quad (53)$$

and

$$\frac{1}{2}\hat{X}_a = -15\left\{(\sin \hat{b}) \left[-\gamma + \ln\left(\frac{b}{2a^2}\right) + 2 Ci(\hat{b}) - Ci(2\hat{b}) \right] - (\cos \hat{b}) [2 Si(\hat{b}) - Si(2\hat{b})] - 2 Si(\hat{b}) \right\}, \quad (54)$$

where \hat{b} is the dipole length kb in electrical radians (b being the dipole length in meters), \hat{a} is the dipole radius ka in electrical radians (a being the dipole radius in meters), $a/b \ll 1$, γ is Euler's constant (0.5772), and $S_1(x)$, $Ci(x)$, and $Si(x)$ are defined as

$$S_1(x) = \int_0^x \frac{1 - \cos y}{y} dy, \quad (55a)$$

$$Ci(x) = \int_x^\infty \frac{\cos y}{y} dy, \quad (55b)$$

and

$$Si(x) = \int_0^x \frac{\sin y}{y} dy. \quad (55c)$$

The normalized values of antenna impedance

$$R_a + jX_a = 1 + j\hat{X}_a/\hat{R}_a \quad (56)$$

do not depend on the current point on the antenna chosen for reference.

The characteristics of the surface wave obtained from the solution of the dispersion relation (19) may be displayed in various ways. Perhaps the most universal way is a wavenumber diagram: kD vs ξ_s . For convenience of scale in Fig. 7 to follow, these parameters will be divided by 2π to obtain D/λ and D/λ_g (fractional wavelengths).

The general features of the wavenumber diagram are well known [4], and special aspects for the case of the normal Yagi structure ($\theta_0 = 90^\circ$) are discussed by Mailloux [21]. In particular Mailloux discusses the possibility of wave solutions for antennas of length $\lambda/2 < b < \lambda$ (inductive antennas). He concludes that the antennas must be capacitive to support a surface wave. The present computations, shown in Fig. 7, agree with those of Mailloux and confirm this conclusion for the case $\theta_0 = 90^\circ$. The region of capacitive antenna length, approximately $b/\lambda < 0.5$, is restricted to a region of each diagram that is below

$$\frac{D}{\lambda} = \frac{b}{\lambda} \frac{D}{b} = 0.5 \frac{D}{b}. \quad (57)$$

For example, in Fig. 7a this capacitive region is below $D/\lambda = 0.5 D/b = 0.5 (0.200)/0.300 = 0.33$.

However, when $\theta_0 \neq 0$, it is evident just from the *form* of the imaginary part of $Q(\xi)$, given by (52c), that inductive dipoles will generally lead to solutions for some θ_0 less than 90° ; unless $u(\xi) \equiv 0$, $\text{Im } Q(\xi)$ will change sign as $\theta_0 \rightarrow 0$. Figure 7 shows wave solutions when $b/\lambda > 0.5$ for $\theta_0 = 30^\circ$ and 0° . In the computations (Fig. 7) the mutual coupling between antennas has (apart from a scale factor) been approximated by the mutual impedance between canonical-minimum-scattering antennas having the radiation pattern (in the open-circuited-array environment) of short dipoles (Eqs. (34) and (52)). Therefore results obtained for inductive dipoles apply, strictly speaking, only to short inductively loaded dipoles. Because of the slow change of the radiation pattern with dipole length, however, the theory of mutual coupling between minimum-scattering antennas [17] indicates that these results are approximately applicable to arrays of (unloaded) dipoles somewhat longer than $1/2$ wavelength. In Fig. 7 the input impedance given by (53) and (54) is specified in terms of a fixed dipole length b , fixed dipole radius a , and the free-space wavelength λ . Of course the form of (54) plays a large role in determining the frequency dependence shown.

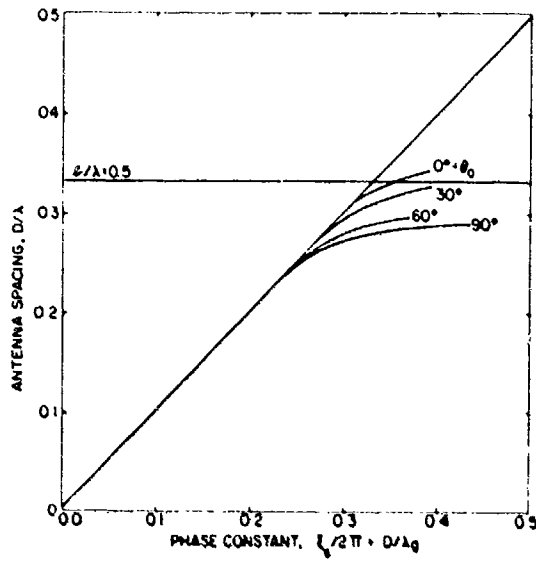
A part of the active impedance $\text{Re } Q(\xi)$ in the range $0 < |\xi| < kD$, although it does not enter into the resonance calculations ($\text{Re } Q(\xi) \equiv 0$, $kD < |\xi| < \pi$), is readily compared for short and $1/2$ -wavelength dipoles. This portion of the active-impedance summation can be rigorously expressed in terms of the radiation patterns [12]

$$\text{Re } \hat{Q}(\xi) = \frac{2\pi R_0}{kD} \int_0^{2\pi} d\phi P_a \left[\cos^{-1} \left(\frac{\xi}{kD} \right), \phi \right], \quad (58)$$

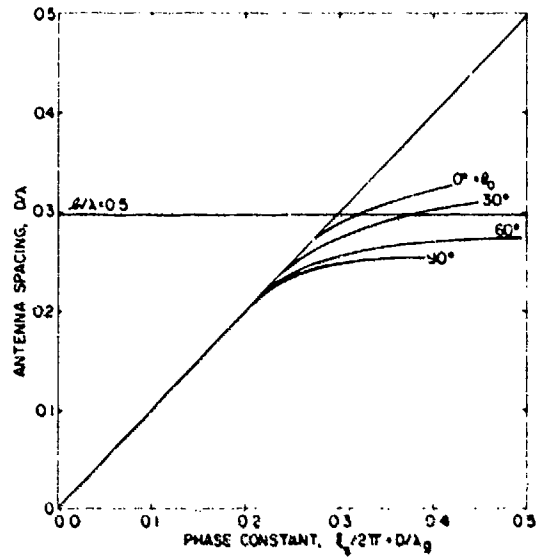
where R_0 is the input resistance to the antenna element in the open-circuited array environment. For a CMS antenna $R_0 \equiv R_{\text{CMS}}$, which has been normalized to 1. In (58) $P_a(\theta, \phi)$ is the radiation pattern of an element in the open-circuited-array environment, normalized to unit radiated power. For the readily computed special case of collinear dipoles ($\theta_0 = 0$)

$$\text{Re } Q(\xi) = \frac{3}{2} \frac{\pi}{kD} \left[1 - \left(\frac{\xi}{kD} \right)^2 \right] \quad (59)$$

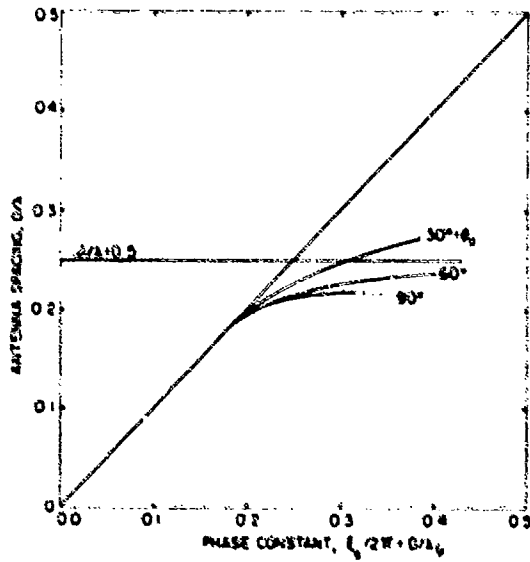
for short dipoles (52a) and



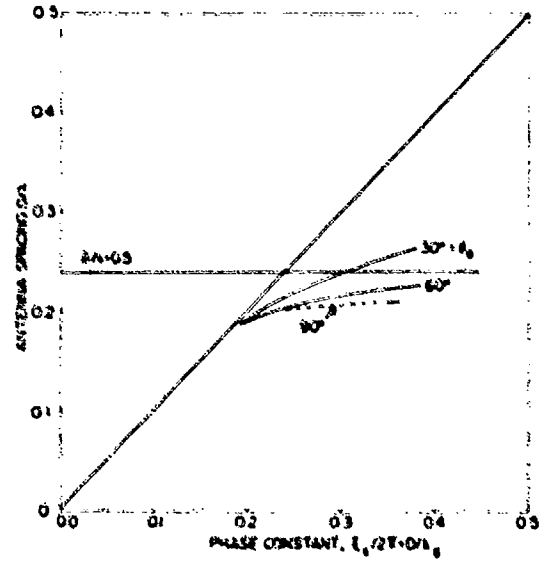
(a) Dipole length $b = 0.300$ m



(b) Dipole length $b = 0.340$ m



(c) Dipole length $b = 0.400$ m



(d) Dipole length $b = 0.420$ m

Fig. 7 — Wavenumber diagrams for a surface wave on an infinite Yagi structure with a dipole radius $a = 0.00635$ m, a dipole spacing $D = 0.200$ m, and various inclination angles θ_0

$$\operatorname{Re} Q(\xi) = \frac{4\pi}{7.658} \frac{\pi}{kD} \frac{\cos^2\left(\frac{\pi\xi}{2kD}\right)}{1 - \left(\frac{\xi}{kD}\right)^2} \quad (60)$$

for half-wave dipoles [12,17,19]. (In (60) an error in the coefficient of the corresponding expression (37) of Ref. 12 and (78) of Ref. 17 has been corrected.) Although the functional form is different, numerically the patterns and consequent variations of $\operatorname{Re} Q(\xi)$ are similar. In the range $0 < |\xi| < 0.6 kD$ the two differ by less than 10%.

Figure 8 illustrates several features of significance in the computations. The first feature is the dependence of the active reactance $\operatorname{Im} Q(\xi)$ on ξ . The second is the solution of the resonance relation ξ_s at the intersection of the negative-antenna-reactance ($-X_a$) line with the active-reactance line. The third is the extreme sensitivity of the solution (ξ_s) to small changes in antenna reactance for larger values of ξ_s (the slowest waves). Because of this sensitivity the solution becomes unreliable; hence the dispersion curves in Fig. 7 have been broken off.

Independent results with which the present theory may be compared are available for only the conventional Yagi structure, with $\theta_0 = 90^\circ$, and consequently only for antenna reactances corresponding to inductive dipole lengths $b < \lambda/2$. A comparison with the theory of Mailloux [7] is shown in Fig. 9. The relatively simple expression for antenna reactance used (Eq. (54)) is at about the limit of its range of validity in terms of dipole radius [19].

A possible application of the new information on Yagi structures contained in Fig. 7 is in design of a mechanically compensated broadband Yagi antenna. The well known condition for optimum directivity of a Yagi surface-wave antenna (Hansen-Woodyard) is cited by Ehrenspeck and Poehler [9]. In the notation of Fig. 7, the required relation between wavelengths and the length L of the Yagi director array is

$$0.468 \frac{2\pi D}{L} = \frac{D}{\lambda_s} - \frac{D}{\lambda}. \quad (61)$$

In Fig. 10 this relation is shown as the curve labeled "optimum" superimposed on a (schematic) wavenumber diagram for a generalized Yagi structure. As frequency (D/λ) is increased, a conventional director structure ($\theta_0 = 90^\circ$) of fixed dipoles proportioned to satisfy relation (61) (point A) rapidly departs from this condition to point B. However, if each dipole is rotated appropriately to an inclination $\theta_0 < 90^\circ$, the optimum relation is restored at the higher frequency (point C). Thus a director array of dipoles, mechanically ganged so that frequency and inclination track, produces optimum performance of the director at each frequency. However, the concomitant rotation of the element pattern for each dipole does involve some loss of directivity.

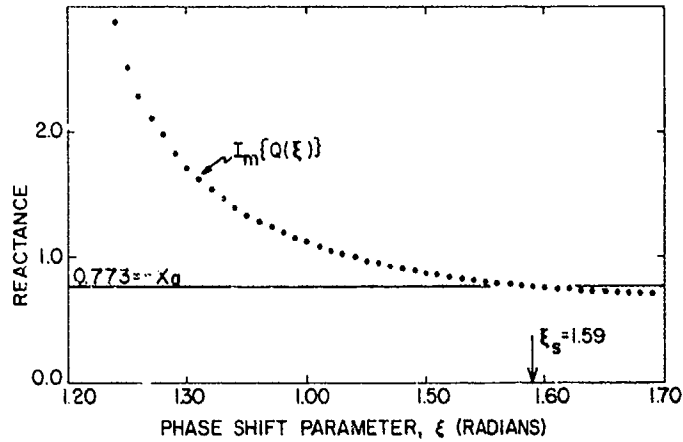


Fig. 8. — Calculated effects of the surface-wave phase-shift-parameter root ξ_s for a conventional Yagi structure ($\theta_0 = 90^\circ$) with $a = 0.00635$ m, $b = 0.440$ m, $D = 0.200$ m, and $D/\lambda = 0.196$ ($kD = 1.23$)

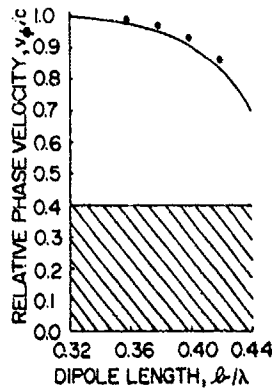


Fig. 9 — Comparison of the relative phase velocity of a surface wave from the theory of Mailoux [7] (solid curve) and from the present analysis (points)

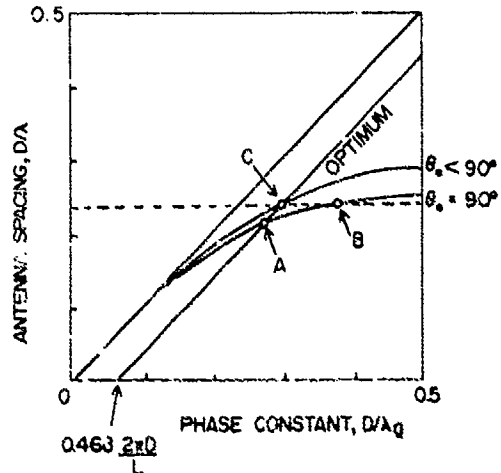


Fig. 10 — Rotation of the dipole inclination θ_0 required for frequency (D/λ) compensation of a Yagi director array. When θ_0 is 90° and performance is optimum for a first frequency (point A), the performance is not optimum for a higher frequency (point B). However, decreasing the dipole inclination to an angle $\theta_0 < 90^\circ$ would again give optimum performance (point C) at the higher frequency.

ACKNOWLEDGMENTS

The work reported here was sponsored by the Naval Air Systems Command under the direction of Mr. Robert Thyberg and Mr. J. Tyszkiewicz. The author is grateful to Dr. T. L. ap Rhys for his interest and valuable comments.

REFERENCES

1. S. Uda, "Short Wave Projector — Historical Records of My Studies in Early Days," privately printed, 1974, Japan, Chapter I.
2. H. Yagi and S. Uda, "Projector of the Sharpest Beam of Electric Waves," Proc. Imperial Academy 2 (No. 2), 1926.
3. H.W. Ehrenspeck and H. Poehler, "A New Method for Obtaining Maximum Gain from Yagi Antennas," IRE Transactions on Antennas and Propagation AP-7, 379-386 (Oct. 1959); presented at WESCON 1956, Los Angeles.
4. R.E. Collin and F.J. Zucker, *Antenna Theory*, Part II, McGraw-Hill, New York, 1969, Chapter 19, by A. Hessel, "General Characteristics of Traveling Wave Antennas," pp. 151-258, and Chapter 21 by F. J. Zucker, "Surface-Wave Antennas" pp. 298-348. (These chapters contain extensive lists of references.)
5. D.L. Sengupta, "On the Phase Velocity of Wave Propagation along an Infinite Yagi Structure," IRE Transactions on Antennas and Propagation AP-7, 234-239 (July 1959).
6. R.J. Mailloux, "Excitation of a Surface Wave along an Infinite Yagi-Uda Array," IEEE Transactions on Antennas and Propagation AP-13, 719-724 (Sept. 1965).
7. R.J. Mailloux, "The Long Yagi-Uda Array," IRE Transactions on Antennas and Propagation AP-14, 128-137 (Mar. 1966).
8. R.W.P. King and S.S. Sandler, "The Theory of Endfire Arrays," IEEE Transactions on Antennas and Propagation AP-12, 276-280 (May 1964).
9. A.C. Gately, Jr., D.J.R. Stock, and E. Ru-Shao Cheo, "A Network Description for Antenna Problems," Proceedings IEEE 56, 1181-1193, (July 1968).
10. W.K. Kahn and H. Kurs, "Minimum Scattering Antennas," IEEE Transactions on Antennas and Propagation AP-13, 671-675 (Sept. 1965).
11. W.K. Kahn and W. Wasykiwskyj, "Coupling, Radiation and Scattering by Antennas," Proceedings M.R.I. Symposium on Generalized Networks, Vol XVI, Polytechnic Institute of Brooklyn, Apr. 1966, pp. 83-114.
12. W. Wasykiwskyj and W.K. Kahn, "Mutual Coupling and Element Efficiency for Infinite Linear Arrays," Proceedings IEEE 56, 1901-1907 (Nov. 1968).
13. W. Wasykiwskyj and W.K. Kahn, "Infinite Arrays of Sub-Array Antennas," pp. 83-90 in *Phased Array Antennas*, A.A. Oliner and G.H. Knittel, editors, Archtech House, Dedham, Mass., 1972.
14. L.A. Hazeltine, "Means for Eliminating Magnetic Coupling between Coils," U.S. Patent 1,577,421, Mar. 16, 1926.

15. U. Grenander and G. Szego, *Toeplitz Forms and Their Applications*, University of California Press, Berkeley, 1958.
16. A.A. Oliner and R.G. Malech, Chapter 3 in *Microwave Scanning Antennas*, R.C. Hansen, editor, Vol. II, Academic Press, New York, 1966.
17. W. Wasylkiwskyj and W.K. Kahn, "Theory of Mutual Coupling Among Minimum-Scattering Antennas," *IEEE Transactions on Antennas and Propagation* AP-18, 204-216 (Mar. 1970).
18. M. Abramowitz and I. Stegun, editors, *Handbook of Mathematical Functions*, Dover, New York, 1964, Chapter 10, pp. 437-442.
19. E.C. Jordan, *Electromagnetic Waves and Radiating Systems*, Prentice-Hall, Englewood Cliffs, N.J., 1950, Section 11.05, pp. 359-364.
20. E.C. Jordan and K.G. Balmain, *Electromagnetic Waves and Radiating Systems*, 2nd Edition, Prentice-Hall, Englewood Cliffs, N.J., 1968.
21. R.J. Mailloux, "A Unification of Antenna Theory and Wave Theory: Infinite Yagi-Uda Arrays," Technical Report 451, Cruft Laboratory, Harvard University, Cambridge, June 22, 1964.
22. L.B. Felsen and W.K. Kahn, "Transfer Characteristics of 2N-Port Networks," *Proceedings of the Symposium on Millimeter Waves, MRI Symposium IX*, Polytechnic Press, New York, 1960, pp. 477-512.

APPENDIX

The Functional Forms of $Q(\xi)$ and $q(\xi)$

Symmetry and Lorentz reciprocity result in relation (4) among the impedance coefficients:

$$Z_{\nu} = Z_{-\nu} . \quad (A1)$$

As a result the active impedance as given by (14) becomes

$$Q(\xi) = Z_0 + \sum_{\nu=1}^{\infty} Z_{\nu} \cos \nu\xi . \quad (A2)$$

Consequently, if the equation

$$jX_0 + Q(\xi) = 0 \quad (A3)$$

has a root $\xi_s^{(p)}$, then it has another root $\xi_s^{(-p)}$ such that

$$\xi_s^{(-p)} = -\xi_s^{(p)} . \quad (A4)$$

This is a general feature of periodic reciprocal structures [4,22].

If the complex variable $\zeta = \eta e^{j\xi}$ is introduced, the complex active impedance function

$$q(\zeta) = \sum_{\nu=-\infty}^{\infty} Z_{\nu} \zeta^{-\nu} \quad (\text{A5a})$$

can be put into the form

$$q(\zeta) = Z_0 + \sum_{\nu=1}^{\infty} Z_{\nu} (\zeta^{\nu} + \zeta^{-\nu}). \quad (\text{A5b})$$

Consequently, if the equation

$$jX_a + q(\zeta) = 0 \quad (\text{A5})$$

has a root $\zeta_s^{(p)}$, then it has another root $\zeta_s^{(-p)}$ such that

$$\zeta_s^{(-p)} = \frac{1}{\zeta_s^{(p)}}. \quad (\text{A7})$$

The active impedance (A2) can be summed in closed form for an array of dipoles inclined at the special angle $\sin^2 \theta_0 = 2/3$, at which angle Z_{ν} reduces to (37), which by use of (35a) is

$$Z_{\nu} = j \frac{e^{-j|\nu|kD}}{|\nu|kD}. \quad (\text{A8a})$$

In the case $\nu = 0$

$$Z_0 = 1. \quad (\text{A8b})$$

The remainder of this appendix deals only with this special angle. Substituting (A8a) and (A8b) in (A2), one has

$$Q(\xi) = \frac{j}{kD} \sum_{\nu=1}^{\infty} \frac{e^{-j\nu(kD - \xi)}}{\nu} + 1 + \frac{j}{kD} \sum_{\nu=1}^{\infty} \frac{e^{-j\nu(kD + \xi)}}{\nu}. \quad (\text{A9})$$

If k is assumed to have a small, negative imaginary part, so that

$$k = k_r + jk_i, \quad k_i < 0, \quad (\text{A10})$$

then the series

$$\sum_{\nu=0}^{\infty} e^{-j\nu(kD - \xi)} = \sum_{\nu=0}^{\infty} (\sigma \zeta)^{\nu} \quad (\text{A11})$$

is absolutely convergent. Integrating term by term (limits 0 and $\sigma\xi$) yields the first summation in (A9). On the other hand (A11) is a geometric progression with the sum

$$\frac{1}{1 - \sigma\xi}. \quad (\text{A12})$$

Consequently the first sum in (A9) is also given by the integral of (A12):

$$\int_0^{\sigma\xi} \frac{dx}{1-x} = -\ln(1 - \sigma\xi), \quad (\text{A13})$$

in which $\ln \xi'$ denotes the natural logarithm of ξ' . The expression (A13) for the sum is a multivalued function of $\sigma\xi$, since $\ln \xi'$ is multivalued. But the sum (A11) is single valued; it converges to the principal value of the logarithmic function $\text{Ln } \xi'$ defined by

$$-\pi < \text{Im}(\text{Ln } \xi') < +\pi. \quad (\text{A15})$$

The second summation in (A9) may be performed similarly. The complete result is

$$q(\xi) = -\frac{j}{kD} \text{Ln}(1 - \sigma\xi) + 1 - \frac{j}{kD} \text{Ln}\left(1 - \frac{\sigma}{\xi}\right). \quad (\text{A16})$$

In the limit $k_f \rightarrow 0$

$$q(\xi) = q(e^{j\xi}) = Q(\xi). \quad (\text{A17})$$

In the main text the finite Fourier transform was employed to obtain a formal solution of the difference equation (5) for the (Green's function) currents I_n . The result is

$$I_n = \frac{1}{2\pi} \int_{-\pi}^{\pi} \frac{E_g e^{-jn\xi}}{jX_a + Q(\xi)} d\xi, \quad (\text{A18})$$

where the value of Q in (15) has been set equal to zero and this superscript suppressed. This solution was obtained without explicit reference to boundary conditions (in this case conditions at $|n| \rightarrow \infty$.) Without such boundary conditions or their equivalent, any solution of the homogeneous difference equation may be added to a given solution for the currents, producing another solution. This lack of uniqueness manifests itself through the presence of singularities on the path of integration. One might intuitively associate a zero of the denominator with finite I_n even for $E_g \rightarrow 0$, that is, with solutions of the homogeneous equation.

A unique solution is obtained when nonzero solutions of the homogeneous equations are excluded by introducing dissipation. Some dissipation, no matter how little, is physically unavoidable; therefore this process selects the physically correct unique solution in the

limit as the dissipation approaches zero. In terms of the singularities of (A18), dissipation removes these singularities from the real path of integration $-\pi < \xi \leq \pi$ to complex values. The movement of the singularities will now be studied in the complex ζ plane.

The singularities in the integrand of (40a) are the branch points of $q(\zeta)$: roots of $jX_a + q(\zeta) = 0$ and singularities of $\zeta^{-(n+1)}$. The branch points of the function $q(\zeta)$ arise from branch points of $\text{Ln } (\zeta')$ in (A16). These are listed in Table A1. As is well known, dissipation produces a negative imaginary component in k , so that (A10) applies. The effect is to move the branch points $1/\sigma$ and σ off the unit circle:

$$|1/\sigma| = |e^{jkD}| = e^{-k_i D} > 1 \quad (\text{A19a})$$

and

$$|\sigma| = |e^{-jkD}| = e^{k_i D} < 1. \quad (\text{A19b})$$

Table A1 — Branch Points of the Active Impedance Function $q(\zeta)$

Branch Points of $\text{Ln } \zeta'$	Branch Points of $q(\zeta)$
$\zeta' = 1 - \sigma\zeta = 0$	$\zeta = 1/\sigma$ } branch cut
$\zeta' = 1 - \sigma\zeta \rightarrow \infty$	
$\zeta' = 1 - \sigma/\zeta = 0$	$\zeta = \sigma$ } branch cut
$\zeta' = 1 - \sigma/\zeta \rightarrow \infty$	

Properties of the roots of (A3) and (A4) have already been discussed. Displacement of the roots is readily calculated when dissipation is introduced in the form of a (small) real component in the antenna self-impedance. Then (A4) becomes

$$R_a + jX_a + q(\zeta) = 0. \quad (\text{A20})$$

Expanding $q(\zeta)$ in a Taylor series about an unperturbed root $\zeta_s^{(p)}$ results in

$$q(\zeta) = q \left[\zeta_s^{(p)} \right] + \left. \frac{dq}{d\zeta} \right|_{\zeta = \zeta_s^{(p)}} \left[\zeta - \zeta_s^{(p)} \right] + \dots \quad (\text{A21})$$

By construction, to first order in $\zeta - \zeta_s^{(p)}$, one has

$$R_a + \frac{dq}{d\zeta} \Big|_{\zeta_s^{(p)}} \left[\zeta - \zeta_s^{(p)} \right] = 0, \quad (\text{A22a})$$

or

$$\zeta - \zeta_s^{(p)} = -R_a \left(\frac{dq}{d\zeta} \right)_{\zeta_s^{(p)}}^{-1}. \quad (\text{A22b})$$

The right-hand side of (A22b) has been evaluated in another connection; from (26a) and (43), with $n = -1$, the result is

$$\zeta - \zeta_s^{(p)} = R_a k D \zeta_s^{(p)} \frac{\cos kD - \cos \zeta_s^{(p)}}{\sin \zeta_s^{(p)}}. \quad (\text{A23})$$

In (A23), for $p = +1$

$$kD < \zeta_s^{(1)} < \pi \quad (\text{A24a})$$

and for $p = -1$

$$-\pi < \zeta_s^{(-1)} < kD. \quad (\text{A24b})$$

The trigonometric factor is positive in the case of (24a) and negative in the case of (24b). Consequently the root $\zeta_s^{(1)}$ moves radially outward (along $\zeta_s^{(1)}$) and the root $\zeta_s^{(-1)}$ moves radially inward (along $-\zeta_s^{(-1)}$). The location of the singularities in the presence of dissipation is illustrated in Fig. A1.

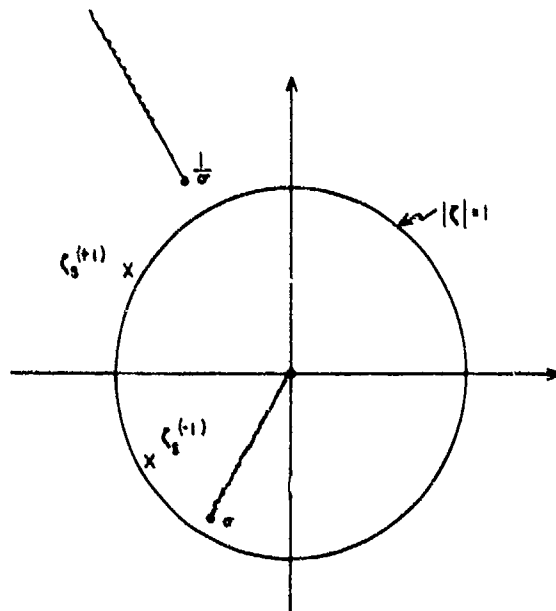


Fig. A1 - Singularities of the integrand in (40a) in the complex ζ plane in the presence of dissipation when $\sin^2 \theta_0 = 2/3$